

RSC Advances



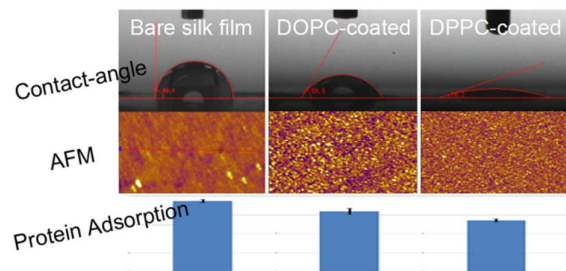
This is an *Accepted Manuscript*, which has been through the Royal Society of Chemistry peer review process and has been accepted for publication.

Accepted Manuscripts are published online shortly after acceptance, before technical editing, formatting and proof reading. Using this free service, authors can make their results available to the community, in citable form, before we publish the edited article. This *Accepted Manuscript* will be replaced by the edited, formatted and paginated article as soon as this is available.

You can find more information about *Accepted Manuscripts* in the [Information for Authors](#).

Please note that technical editing may introduce minor changes to the text and/or graphics, which may alter content. The journal's standard [Terms & Conditions](#) and the [Ethical guidelines](#) still apply. In no event shall the Royal Society of Chemistry be held responsible for any errors or omissions in this *Accepted Manuscript* or any consequences arising from the use of any information it contains.

Table of Contents



Self-assembled lipid membrane provides a smooth, hydrophilic and biocompatible surface coating film for materials.



Journal Name

ARTICLE

Self-assembly of Monolayered Lipid Membranes for Surface-coating of a Nanoconfined Bombyx Mori Silk Fibroin Film

Fan Xu,^a Meimei Bao,^{b,c} Longfei Rui,^{b,c} Jiaojiao Liu,^{b,c} Jingliang Li,^e Yujiang Dou,^d Kai Yang,^{b,c} Bing Yuan,^{b,c,*} and Yuqiang Ma^{a,b,c,*}

Received 00th January 20xx,
Accepted 00th January 20xx

DOI: 10.1039/x0xx00000x

www.rsc.org/

Regenerated *Bombyx mori* (*B. mori*) silk fibroin is a type of widely used biomaterial. The β -sheet structure of it after methanol treatment provides water-insolubility and mechanical stability while on the other side leads to a hydrophobic surface which is less preferred by biological systems. In this work we prepare a novel type of nanoconfined silk fibroin film with a thickness beneath 100 nm. The film has a flat while hydrophobic surface because of its β -sheet structure due to the z-direction confinement during formation. Different types of lipid monolayers, DOPC, DPPC and MO, are assembled on the silk film surface. The lipid coating, especially the DPPC membrane, provides a much smoother and more hydrophilic surface due to the gel phase tails of lipids, in comparison with the DOPC and MO ones which are in a liquid phase and have a much stronger interfacial association between silk film surface and lipid tails. Such lipid coating preserves the biocompatibility and cellular affinity of the silk film which promises potential applications as surface coating for materials for biological use.

1. Introduction

Self-assembly of phospholipid on solid substrates has been widely used to fabricate artificial biomembrane model systems.¹ The presence of a supporting substrate stabilizes a membrane over days and enhances the membrane's mechanical strength while maintaining fluidity.^{2,3} The surface structure and properties of a solid substrate significantly determine the self-assembly process, structure and functional activity of the supported lipid membranes.^{4,5} Based on such a platform, lipid molecular mobility, membrane topography, integration of protein in membrane and Bio-Nano interfacial interaction are widely studied.^{6,7} On the other hand, due to the amphipathicity and biocompatibility of lipid molecules, lipid membrane has been regarded as one of the promising coating surface for biomaterials especially those with hydrophobic surfaces, in case of protein adsorption and immunologic rejection after implantation.^{8,9} Furthermore, the myelin basic protein adsorption can even be controlled by lipid domains.¹⁰

B. mori silk fibroin has been used to fabricate a variety of biomaterials because of its impressive mechanical properties, environmental stability, biocompatibility and

biodegradability.¹¹⁻¹³ Numerous studies have been focused on applications of silk fibroin in the forms of nanofiber, film and three dimensional (3D) matrix.¹⁴⁻¹⁸ Besides that, patterned silk biomaterials are excellent substrates for directing cellular morphology changes and biological functions.^{19,20} The structure and properties of fibroin films can be modified with simple physical or chemical treatments such as stretching, thermal treatment and immersing into selected organic solvents.^{21,22} Regenerated *B. mori* fibroin films primarily consist of random coil and α -helix structures and therefore are soluble in water.²³ As the conformation of a *B. mori* fibroin film is changed to β -sheet structure by methanol treatment, the film becomes water-insoluble hence more stable but less preferred by biological systems.^{24,25} In this context, different approaches such as surface modification with polymer molecules and blending with other macromolecules have been developed to improve the biological performance of silk fibroin films.^{12,26,27}

Regeneration of silk fibers on nanoscale can be endowed with outstanding mechanical properties due to the self-organization of silk fibroin protein with molecular and supramolecular ordering and orientation under geometrically confinement environments.¹⁸ In this study, we aim at understanding the influence of a one dimensionally confined space on the structure and properties of the *B. mori* silk fibroin film, and the surficial coating of it with different types of lipid membranes for biological use. Atomic force microscopy (AFM) was used especially for the study of membrane morphology and domain structure.^{28,29} Along with X-ray diffraction (XRD) and Fourier transform infrared spectroscopy (FTIR) characterizations, it is found that the silk film formed within

^a National Laboratory of Solid State Microstructures and Department of Physics, Nanjing University, Nanjing, 210093, P. R. China. E-mail: xfjhd@126.com,

^b Center for Soft Condensed Matter Physics and Interdisciplinary Research, Soochow University, Suzhou, 215006, P. R. China.

^c College of Physics, Optoelectronics and Energy, Soochow University, Suzhou, 215006, P. R. China.

^d School of Electronic and Information Engineering, Soochow University, Suzhou, 215006, P. R. China.

^e Institute for Frontier Materials, Deakin University, Waurn Ponds, Vic, 3216, Australia.

*Corresponding Authors, E-mail: yuanbing@suda.edu.cn, myqiang@nju.edu.cn

nanoconfined space has a larger content of β -sheet structure. In contrast, the bulk film contains a majority of α -helix. The films formed under confinement also have flat and hydrophobic surface, probably due to its β -sheet structure. The silk films were used as substrate to assemble different types of lipid molecules and the functional films were examined for their protein and cell adsorption properties. It was observed that the surface morphology and chemical property of the silk film, as well as the molecular structure of the lipid molecules, determine the structure and diffusion behavior of lipid membrane supported on it. The assembled lipid layers offer different surface properties which consequently influence the protein and cell adsorption behaviors, which promise potential applications as surficial coating method for biomaterials.

2. Experimental Section

2.1 Materials

1,2-Dioleoyl-sn-glycero-3-phosphocholine (DOPC), 1,2-dipalmitoyl-sn-glycero-3-phosphocholine (DPPC), and 1,2-dipalmitoyl-sn-glycero-3-phosphoethanolamine-N-(lissaminerhodamine B sulfonyl) (Rh-PE) were purchased from Avanti Polar Lipids and used as received. 1-Oleoyl-rac-glycerol (MO) was purchased from Sigma-Aldrich. Bovine serum albumin (BSA) was purchased from Biosharp. Human gastric cancer cell (MGC-803) was purchased from the Type Culture Collection of the Chinese Academy of Sciences, Shanghai, China. The other chemicals were purchased from Shanghai Chemical Reagents Company.

Cover glass substrates (Fisher Brand microscope cover glass) were cleaned in ethanol and acetone separately with ultrasonic. Milli-Q water was used to rinse the substrates extensively before they were dried under nitrogen. The root-mean-square (rms) roughness of the substrates prepared following this procedure was 0.3 ± 0.1 nm as determined by AFM measurement.

Preparation of *B. mori* silk fibroin solution. The silk fibroin solution was prepared according to the procedures reported.¹⁸ Firstly, to degum silk fibers, 20 g of silk cocoons were boiled in 1000 mL of Na_2CO_3 solution (0.5 mg mL^{-1}) for 40 min followed by extensive washing with deionized water. The boiling and washing process was repeated 3 times. After that, the degummed silk fibers were dried in vacuum at room temperature. 20 mL of a ternary solvent containing CaCl_2 /ethanol/water at a weight ratio of 1/2/8 was preheated and maintained at 72°C . 2 g of the degummed silk fiber was cut into small pieces and added to the solvent under vigorous stirring. A viscous light yellow coloured silk protein solution was obtained after 2-3 hours. The solution was then dialyzed using Dialysis Cassettes (MW 3500) for 3 days to remove the impurities, and centrifuged at 10000 rpm for 3 min at 0°C . The supernatant solution was further filtrated and stored at 4°C for use up to 10 days. The final concentration of the obtained silk fibroin solution was $\sim 2 \text{ wt}\%$.

2.2 Preparation of Silk Fibroin Film and Supported Lipid Membranes

One piece of poly(dimethylsiloxane) (PDMS) slice, with a thickness of around 0.5 mm and a size of about $1.5 \times 1.5 \text{ cm}^2$ was fabricated with the traditional spin-coating method. An amount of 50 μL silk fibroin solution was dropped onto a clean glass coverslip. Then the PDMS slice was covered carefully onto it and much of the solution was pressed out from under the slice. The solution was completely dried for 24 hours at room temperature and the silk films, both confined (under the PDMS slice, with a pressure of around $5 \times 10^{-4} \text{ N cm}^{-2}$) and unconfined (around the slice), were obtained after peeling off the PDMS slice from the surface. The as-prepared silk film was immersed into 60% (v/v) aqueous methanol for 30 min, then washed and dried under nitrogen gas.

Supported DOPC, DPPC and MO membranes on the silk film surface were prepared by the traditional Langmuir-Blodgett (LB) deposition method with a KSV NIMA Langmuir-Blodgett instrument (KN2002, KSV, Helsinki).³⁰ In short, the trough of the instrument was first thoroughly cleaned with chloroform and ethanol and completely rinsed with Milli-Q water. It was then filled with fresh water for use as a subphase for the lipid molecules. The silk film substrate was submerged vertically into the subphased water before the induction of lipid. On the other side, the lipid was pre-dissolved in chloroform at 0.2 mg mL^{-1} (1.0 mg mL^{-1} for MO). A volume of 8 μL of lipid solution was spread onto the water/air interface in the trough. After solvent evaporation, the self-assembled lipid monolayer on the water/air interface was compressed to a surface pressure of 32 mN m^{-1} by decreasing the surface area of the trough at a speed of $40 \text{ cm}^2 \text{ min}^{-1}$ through moving the Teflon barriers. The silk film substrate was then drawn upward at a constant speed of 5 mm min^{-1} and simultaneously the lipid monolayer was transferred to the silk film surface by moving the barriers and keeping the surface pressure at a constant value. For the fluorescence experiments, 0.5 mol % Rh-PE was added to the lipid solution in advance.

2.3 Cell Seeding and Protein Adsorption on the Nanoconfined Silk Fibroin Film and Supported Lipid Membranes

Human gastric cancer cells MGC-803 (6×10^5 cells) were seeded onto the nanoconfined silk fibroin films, both without and with lipid-membrane coating. After 24 h incubation at 37°C under an atmosphere containing 5% CO_2 , pictures were taken with a confocal microscope. Ten randomly chosen fields were analyzed for each sample.

To study the protein adsorption properties, silk films without and with supported lipid membranes, were incubated with 2 mg mL^{-1} BSA for 1 min, respectively. Then, the residual protein concentrations were determined by the BCA assay (Beyotime, Shanghai, China).

2.4 Characterization

AFM images were collected with an Asylum Research MFP-3D-SA atomic force microscope (Santa Barbara, CA) setup in tapping mode in air. Etched silicon probes with a resonant frequency of 280-361 kHz and a spring constant of 30-40 N m^{-1} were used.¹⁸ Powder XRD patterns were gathered on a Bruker

D8-Advance diffractometer and Shanghai Synchrotron Radiation Facility (SSRF). An incident angle of 5° was used and the diffractive signal was collected from 10 to 40° (2θ).³¹ FTIR profiles were collected with a Thermo Nicolet 6700, in a reflection mode. Contact-angle test was performed on a MY-SPCA1 contact angle measuring device. In each test, a drop of purified water was dropped on the horizontal surface of the film and a CCD camera was hired to monitor the droplet's roundness. Baseline circle method was used to access contact angles. Fluorescent recovery after photobleaching (FRAP) test was gathered on a Zeiss LSM 710 inverted confocal fluorescence microscope. Fluorescence integration of the photobleached patches was performed using the LSM software of the microscope. All the experiments were carried out at room temperature of 22°C .

3. Results and Discussion

3.1 Characterizations of Nanoconfined Silk Fibroin Film

Fig. 1a shows a digital image of the as-prepared silk film (without lipid coating) after methanol immersion. The transparent square area in the center of the glass slide, marked with A, refers to the silk film formed within a confined space due to PDMS compressing. The thickness of the film was around 80 ± 20 nm which was reproducible and should be roughly determined by the quantity of the solution and the size and weight of the PDMS slice. The random area around, marked with B, refers to the bulk silk film formed under unconfined condition with a thickness of around a few micrometers. The surface morphology of the silk fibroin films, formed under both unconfined and nanoconfined conditions, was further characterized with AFM as shown in Fig. 1c-d. Fig. 1f shows the height profiles along the red lines in c and d, indicating the comparison in surface roughness between the unconfined and nanoconfined area. Within a similar $10 \times 10 \mu\text{m}^2$ scanning region, the unconfined bulk area has a much rougher surface, with a roughness of around 20 nm, compared with that of the nanoconfined area, with a roughness of only 2 nm. Fig. 1e shows a regional magnification of the nanoconfined film in a $5 \times 5 \mu\text{m}^2$ area. Many ellipsoidal nanostructures can be distinguished (Fig. 1e-inset), which are regularly arranged over the whole film. These ellipsoidal nanostructures are quite similar to those of the silk protein nanofibers fabricated within a nanosized AAO template, which was ascribed as β -sheet crystals of silk fibroin formed during the self-assembly of the protein within a nanoconfined space, and further promoted by exposure to methanol.¹⁸

XRD and FTIR were used to further reveal the structures of the silk fibroin films. Fig. 2a shows the XRD profiles of both bulk and nanoconfined silk fibroin films before and after methanol treatment. The bulk film always show diffraction peaks at around 12 and 19.5° which refer to the existence and survival of α -helix structure in the film even after certain methanol treatment.³² In contrast, no such peaks are observed

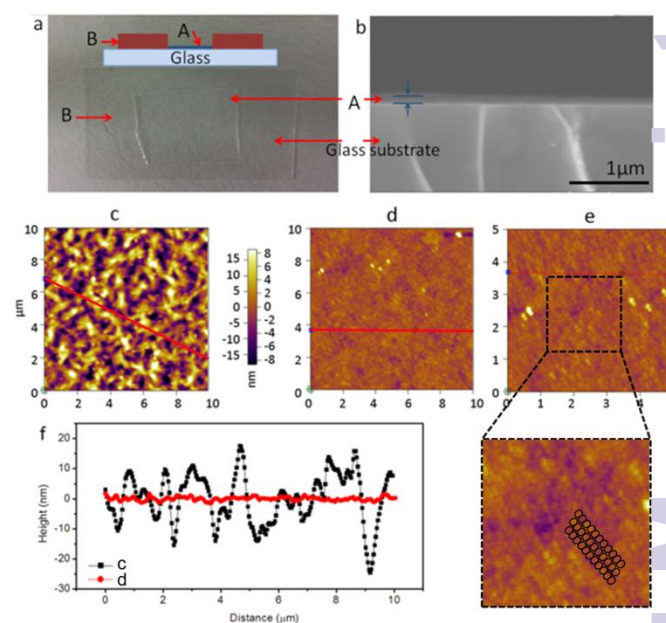


Fig. 1 (a), a digital photo of the silk film supported on a $32 \times 24 \text{ mm}^2$ cover glass. (A) represents the target area of the film, i.e., the confined region by PDMS compressing during film preparation; (B) refers to the unconfined region during film preparation. (b) SEM image of a cross section of the confined film. (c, d), representative AFM images in a $10 \times 10 \mu\text{m}^2$ range of a bulk silk fibroin film and a nanoconfined silk fibroin film. (e), regional magnification of (d) in a $5 \times 5 \mu\text{m}^2$ area. Inset emphasizes a schematic distribution of the ellipsoidal nanostructures over the film. (f), line profiles taken from images (c) and (d). The vertical distance was measured using the analysis associated with the AFM. Black stands for the bulk silk film (c) and red stands for the nanoconfined silk film (d).

for the nanoconfined films, indicating that α -helix structure does not exist in the films. FTIR spectra have been shown to be sensitive to the molecular structure of silk fibroin materials. As shown in Fig. 2b, the bulk film sample before methanol treatment shows strong bands at 1641 , 1531 and a shoulder at 1267 cm^{-1} , assigned to α -helix, and 1620 , 1514 and 1235 cm^{-1} , assigned to β -sheet.³² After methanol treatment, the strong peaks at 1641 and 1531 cm^{-1} greatly moved to 1620 and 1514 cm^{-1} , respectively, indicating the significant transformation from α -helix to β -sheet within the film. However, for the nanoconfined films both before and after methanol treatment, the α -helix peaks or shoulders are always indistinguishable while the β -sheet ones remain strong. This means that the α -helix structure hardly exists in the nanoconfined film, which is in consistent with the XRD result.

To examine the hydrophobicity of the silk fibroin films formed under nanoconfinement, contact angle measurements were also conducted on the nanoconfined films with and without methanol treatment. As demonstrated in Fig. 2c and d, the contact angle of the nanoconfined silk fibroin film remains unchanged at around $90 \pm 2^\circ$ after being treated with methanol. The surface of such nanoconfined silk fibroin films is relatively hydrophobic due to the β -sheet formation which is consistent with the conclusion from XRD and FTIR results. In contrast, for the unconfined bulk film, the contact angle only

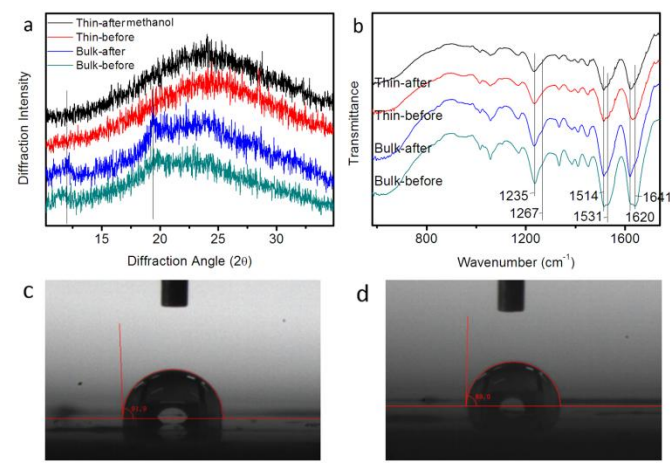


Fig. 2 (a), XRD spectra of the nanoconfined as well as bulk silk fibroin films before/after treated with methanol-water mixtures. Red: nanoconfined silk fibroin film before methanol; Black: after methanol treatment; Green: bulk silk fibroin film before methanol; Blue: after methanol. (b) FTIR spectra of the nanoconfined and bulk silk fibroin films before/after methanol treatment. Colorful lines stand for the same meaning as in (a). (c, d), contact angles of the nanoconfined silk fibroin film before and after treatment with methanol. The angles for both (c) and (d) are $90 \pm 2^\circ$, obtained from 5 different places on the film.

changes from $73 \pm 3^\circ$ to $81 \pm 3^\circ$ after methanol treatment (Supporting Information, Fig. S1). In this way, a compact and somewhat hydrophobic surface is demonstrated for the nanoconfined silk fibroin film, on which assembly of lipid membranes occurs.

3.2 Directed Self-Assembly of Lipid Monolayers on the Nanoconfined Silk Film Surface

A monolayer of lipid molecules was deposited on the surface of nanoconfined film by the traditional LB deposition method. Fig. 3a-i represent the AFM topography images of the supported membranes of three different types of lipids, DOPC, DPPC and MO, respectively. For accuracy, images with the same area are compared among different types of lipid membranes. For example, for the $2 \times 2 \mu\text{m}^2$ images, the DOPC membrane demonstrates rough surface morphology with spherical nanostructures distributed over the film (Fig. 3a). Compared with DOPC, the DPPC membrane presents a much smoother surface with nanostructures of a much smaller size (Fig. 3d). The MO film, in Fig. 3g, demonstrates the morphology as that between the DOPC and DPPC films. The AFM images of the other regions, 5×5 or $10 \times 10 \mu\text{m}^2$, show similar results. Fig. 3j shows the height profiles of all the three types of lipid membranes, from which we can quantitatively obtain the height and size of the nanostructures (i.e. fluctuation period) on them. The standard deviation of DOPC membrane is calculated to be 2.09 ± 0.1 nm, with a nanostructure size of 105 ± 10 nm. The standard deviations of the DPPC and MO films are determined to be 1.44 and 2.07 ± 0.1 nm, with nanostructure sizes of 51 ± 4 nm and 63 ± 4 nm, respectively.

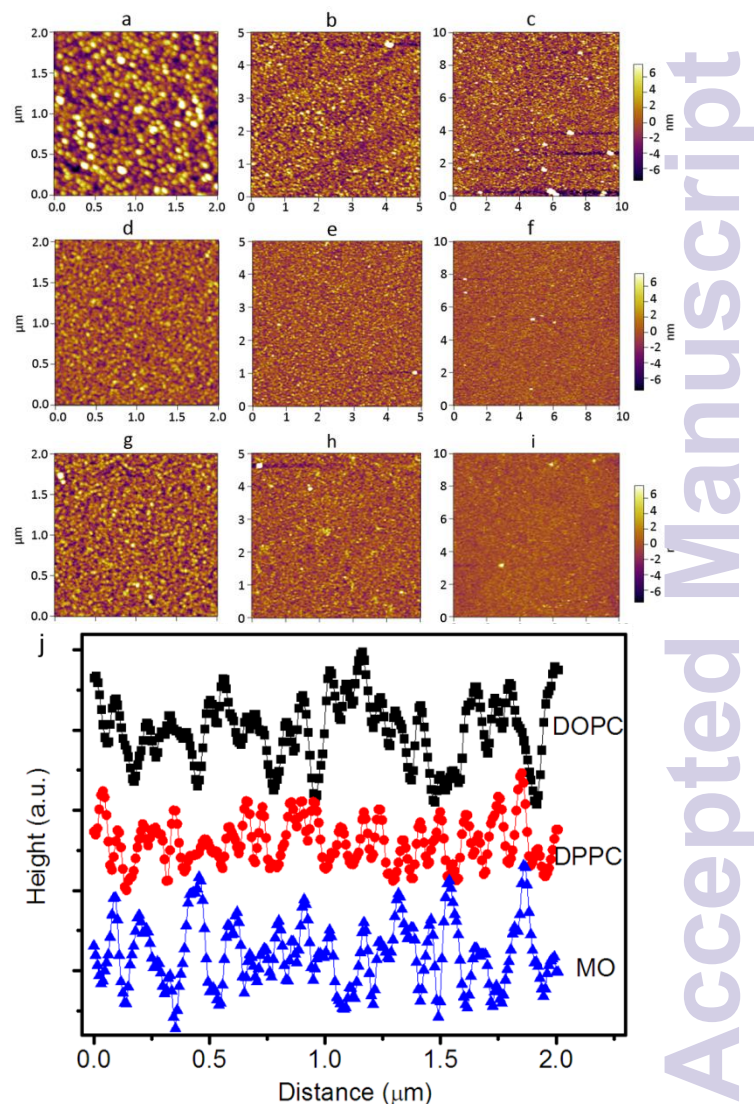


Fig. 3 AFM topography images of the lipid monolayers deposited on the surface of the nanoconfined silk fibroin films. (a-c), DOPC; (d-f), DPPC; (g-i), MO. The images were obtained in a 2×2 (a, d and g), 5×5 (b, e and h), or 10×10 (c, f and i) μm^2 region. (j), line profiles taken from (a), (d) and (g). Black stands for DOPC, red stands for DPPC and blue stands for MO.

The differences in the surface structure of the three lipid membranes might due to the different molecular structure of the lipids, in addition to the surface morphology of the silk film substrate. It is known that the DOPC molecules consist of two hydrophobic unsaturated fatty acid tails which stay in liquid phase at room temperature (Supporting Information, Fig. S2a). The lipid molecules prefer to organize into a somewhat disordered assembly on a hydrophobic surface, with the tails associated directly with the substrate surface.³³ In contrast, the DPPC molecules composed of two saturated fatty acid tails (Supporting Information, Fig. S2b), stay in gel-phase under room temperature. The strong association between adjacent tails ensures the lipids to form a continuous membrane on a substrate surface, with a much reduced fluctuation in comparison with that of DOPC. The MO lipid has only one

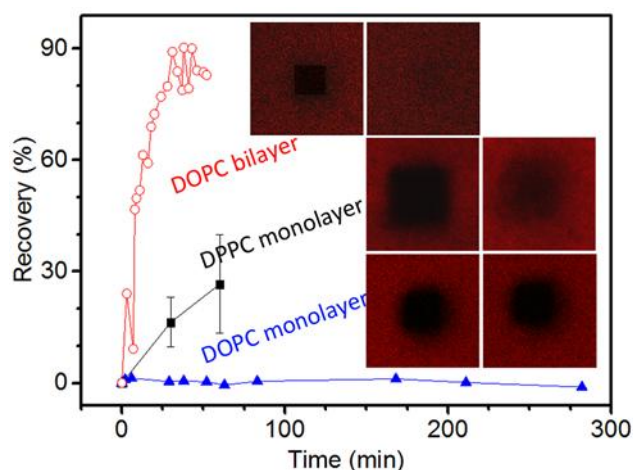


Fig. 4 FRAP of DOPC, DPPC monolayer and DOPC bilayer supported on nanoconfined silk fibroin films in 5 hours.

unsaturated tail (Supporting Information, Fig. S2c), so it fluctuates in a similar way as DOPC but with much smaller sized nanostructures. In a word, a direct and accurate reflection of the morphology of the lipid membranes in response to the lipid structure has been observed, which indicates the intimate association between lipids and the silk substrate surface.³³

Fig. 4 shows the FRAP tests of the DOPC and DPPC membranes supported on the nanoconfined silk fibroin films to show the lateral fluidity of the lipid molecules. For the DOPC monolayer membrane, recovery did not occur even after a long time of 5 h after photobleaching. For the DPPC monolayer film, 30% fluorescence was recovered in around 1 hour. This indicates that strong association has occurred between DOPC molecules and the silk film substrate, which significantly hinders the lateral diffusion of the lipid molecules. However, for the DPPC monolayer membrane, the association is weaker. These results further support our presumptions in the AFM experiments. In a control experiment, we deposited a second monolayer of DOPC on the primary layer of DOPC molecules. More than 90% of the fluorescence of the as-prepared DOPC membrane was recovered within 20 min after photobleaching. This means that a confluent fluidity of the lipid molecules occurs, probably in the upper leaflet, which indicates the silk film supported lipid layer is a good biological substrate.

Contact angle tests were further performed on the silk film supported lipid monolayer membranes as shown in Fig. 5. As mentioned above, the nanoconfined silk fibroin film, both before and after methanol treatment, demonstrates a somewhat hydrophobic surface with a contact angle of around $90 \pm 2^\circ$. After lipid deposition, the surface was changed to be much hydrophilic with a contact angle of around 60° for DOPC and 15° for DPPC membrane. This is reasonable as we have demonstrated that for the DPPC film, a well-organized and continuous membrane covering the silk surface with the

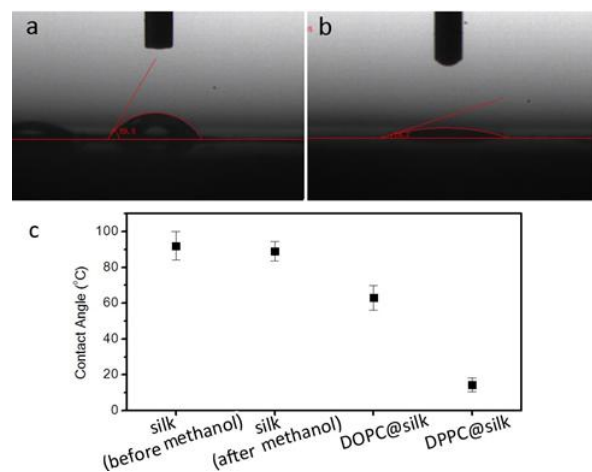


Fig. 5 (a, b), Contact angle tests of DOPC and DPPC monolayer membranes supported on nanoconfined silk fibroin films. (c), summary of the contact angle distribution of different films, including silk film before/after methanol treatment and DOPC/DPPC coated film.

hydrophilic head layer toward the air was formed. In comparison, for the DOPC film, strong association occurs between the disordered DOPC tails and the hydrophobic silk film substrate leading to the exposure of part of the tails to the air. This leads to the result that parts of the membrane's surface is less hydrophilic.

3.3 Protein Adsorption and Cell Incubation on the Lipid Coated Films.

To further confirm the biocompatibility of the lipid monolayer coated silk films, we conduct the traditional Bovine serum albumin (BSA) adsorption and cellular affinity experiments on both the bare silk fibroin film and the lipid coated ones. In the BSA adsorption test, the density of residual protein left in solution in 1 min after immersing the films in the protein solution is used to judge the protein blocking effect of the film surface. For the bare silk film, an average of around $95.25 \pm 0.2\%$ of the protein left (obtained from repeated tests, Fig. S3 in Supporting Information), while for the films coated with DOPC and DPPC, the value was increased to $96.5 \pm 0.4\%$ and $97.9 \pm 0.2\%$, respectively, being even higher than that of bare silk film. This indicates that the assembly of lipid, especially DPPC, further decreased the protein adsorption on the silk film surface. In the cell incubation test all the three types of film substrates, including the bare silk film, DOPC and DPPC coated ones, were immersed in solution containing the same amount of MGC-803 cells and incubated for 24 h before observation. Typical visual field of the substrate after cell adsorption is shown in Fig. S3b-d (Supporting Information). The amount of the cells adherent onto each type of film was analyzed from 10 different positions of each film and triple independent repeated experiments. In an area of $225.4 \times 225.4 \mu\text{m}^2$ region, an average amount of 28 cells is found on the bare silk film surface, while for the DOPC or DPPC coated surface, 18 or 26 cells is observed. This result indicates that the lipid coating

would not much disturb the affinity property of the silk fibroin film to cells.

4. Conclusions

We have demonstrated in this paper the successful assembly of different lipid membranes on the surface of a nanoconfined silk fibroin film. The silk film is formed within a one dimensionally confined space by PDMS compressing and displays a nanoscale flat and hydrophobic surface probably due to the β -sheet structure of it. Monolayers of different types of lipids, DOPC, DPPC and MO are assembled on the silk film surface by the traditional LB deposition method. AFM and contact-angle tests show a smoother and more hydrophilic surface of the DPPC-coated film compared to the films coated with DOPC and MO, probably due to the differences in structures of lipid tails and their interaction with the substrate surface. The DPPC lipids prefer to form a more continuous and smoother coating on the silk film surface due to the gel phase and strong association between adjacent tails within the layer. However, for DOPC, strong association occurs between the much disordered lipid tails and the silk film surface. In the subsequent protein adsorption and cell incubation tests, all the lipid-coated films, especially the DPPC-coated film, show low protein adsorption (even lower than that of the bare silk film) and good cellular affinity effect, indicating good biocompatibility of the lipid-coated surface. These results demonstrate the feasibility of effectively decorating the surface of materials with lipid coating for biological uses.

Acknowledgements

This work was financially supported by the National Science Foundation of China (Nos. 91027040, 31061160496, 21374074, and 21422404), and the National Basic Research Program of China (No. 2012CB821500). B.Y. and K.Y. thank the support of the Natural Science Foundation of Jiangsu Province of China (Nos. BK2012177 and BK20131194). The authors also thank the Small Angle X-ray Scattering Station (BL16B) and X-ray Diffraction Station (BL14B) at Shanghai Synchrotron Radiation Facility (SSRF) for sample characterizations.

Notes and references

- R. P. Richter, R. Bérat and A.R. Brisson, *Langmuir*, 2006, **22**, 3497.
- K. Sugihara, J. Voros and T. Zambelli, *ACS Nano*, 2010, **4**, 5047.
- S. Ahmed, R. R. Madathingal, S. L. Wunder, Y. Chen and G. Bothun, *Soft Matter*, 2011, **7**, 1936.
- D. Keller, N. B. Larsen, I. M. Moller and O. G. Mouritsen, *Phys. Rev. Lett.*, 2005, **94**, 1.
- A. P. Shreve, M. C. Howland, A. R. Sapuri-Butti, T. W. Allen and A. N. Parikh, *Langmuir*, 2008, **24**, 13250.
- R. Tero, *Materials*, 2012, **5**, 2658.
- Y. J. Dou, J. L. Li, B. Yuan and K. Yang, *Appl. Surf. Sci.*, 2014, **296**, 95.
- F. Q. Tang, L. L. Li and D. Chen, *Adv. Mater.*, 2012, **24**, 1504.
- J. J. Liu, N. Y. Lu, J. L. Li, Y. Y. Weng, B. Yuan, K. Yang and Y. Q. Ma, *Langmuir*, 2013, **29**, 8039.
- M. Sublimi Saponetti, M. Grimaldi, M. Scrima, C. Albonetti, S. L. Nori, A. Cucolo, F. Bobba and A. M. D'Ursi, *PLoS One*, 2014, **9**, e115780.
- T. Chirila, Z. Barnard, Zainuddin, D. G. Harkin, I. R. Schwab and L. Hirst, *Tissue Eng. Part A*, 2008, **14**, 1203.
- L. Q. Bai, L. J. Zhu, S. J. Min, L. Liu, Y. R. Cai and J. M. Yao, *Appl. Surf. Sci.*, 2008, **254**, 2988.
- D. N. Rockwood, R. C. Preda, T. Yucel, X. Q. Wang, M. L. Lovett and D. L. Kaplan, *Nat. Protoc.*, 2011, **6**, 1612.
- Y. Kawahara, K. Furukawa and T. Yamamoto, *Macromol. Mater. Eng.*, 2006, **291**, 458.
- R. Nazarov, H. J. Jin and D. L. Kaplan, *Biomacromolecules*, 2004, **5**, 718.
- U. J. Kim, J. Park, H. J. Kim, M. Wada and D. L. Kaplan, *Biomaterials*, 2005, **26**, 2775.
- Y. Z. Wang, D. D. Rudym, A. Walsh, L. Abrahamsen, H. Kim, H. S. Kim, C. Kirker-Head and D. L. Kaplan, *Biomaterials*, 2008, **29**, 3415.
- Y. F. Shi, X. H. Li, G. Z. Ding, Y. J. Wu, Y. Y. Weng and Z. J. Hu, *Macromolecules*, 2014, **47**, 7987.
- B. D. Lawrence, J. K. Marchant, M. A. Pindrus, F. G. Omenetto and D. L. Kaplan, *Biomaterials*, 2009, **30**, 1299.
- H. J. Jin, J. Chen, V. Karageorgiou, G. H. Altman and D. L. Kaplan, *Biomaterials*, 2004, **25**, 1039.
- R. D. B. Fraser and T. P. MacRae, *Academic Press*, New York, 1973, pp95.
- H. Y. Kweon, I. C. Um and Y. H. Park, *Polymer*, 2000, **41**, 736.
- G. R. Plaza, P. Corsini, J. Perez-Rigueiro, E. Marsano, G. V. Guinea and M. J. Elices, *Appl. Poly.*, 2008, **109**, 1793.
- H. Y. Kweon and Y. H. Park, *J. Appl. Poly.*, 1999, **73**, 2887.
- Z. Z. Shao and F. Vollrath, *Nature*, 2002, **418**, 741.
- G. Freddi, M. Tsukada and S. Beretta, *J. Appl. Poly.*, 1999, **71**, 1563.
- H. J. Jin, J. Park, R. Valluzzi, P. Cebe and D. L. Kaplan, *Biomacromolecules*, 2004, **5**, 711.
- D. W. Lee, X. Banquy, K. Kristiansen, Y. Kaufman, J. M. Boggs and J. N. Israelachvili, *Proc. Natl. Acad. Sci.*, 2014, **111**, 768.
- E. I. Goksu, J. M. Vanegas, C. D. Blanchette, W. C. Lin, M. Longo, *BBA-Biomembranes*, 2009, **1788**, 254.
- M. C. Howland, A. R. Sapuri-Butti, S. S. Dixit, A. M. Dattelbaum, A. P. Shreve and A. N. Parikh, *J. Am. Chem. Soc.*, 2005, **127**, 6752.
- H. Zhang, L. Li, F. Dai, H. Zhang, B. Ni, W. Zhou, X. Yang and Y. Wu, *J. Transl. Med.*, 2012, **10**, 117.
- M. Z. Li, W. Tao, S. Kuga and Y. Nishiyama, *Polym. Adv. Technol.*, 2003, **14**, 694.
- L. Rui, J. Liu, J. Li, Y. Weng, Y. Dou, B. Yuan, K. Yang and Y. Q. Ma, *BBA-Biomembranes*, 2015, **1848**, 1203.